Triangle singularity in $\tau^- \to \nu_\tau \pi^- f_0(980)$ $(a_0(980))$ decays

L. R. Dai,[1,2,*] Q. X. Yu,[3,2,†] and E. Oset[2,‡]

[1]*Department of Physics, Liaoning Normal University, Dalian 116029, China*
[2]*Departamento de Física Teórica and IFIC, Centro Mixto Universidad de Valencia-CSIC, Institutos de Investigacíon de Paterna, Aptdo. 22085, 46071 Valencia, Spain*
[3]*College of Nuclear Science and Technology, Beijing Normal University, Beijing 100875, China*

(Received 3 October 2018; revised manuscript received 19 November 2018; published 31 January 2019)

We study the triangle mechanism for the decay $\tau^- \to \nu_\tau \pi^- f_0(980)$, with the $f_0(980)$ decaying into $\pi^+\pi^-$. The mechanism for this process is initiated by $\tau^- \to \nu_\tau K^{*0} K^-$ followed by the K^{*0} decay into $\pi^- K^+$, then the $K^- K^+$ produce the $f_0(980)$ through a triangle loop containing $K^* K^+ K^-$ which develops a singularity around 1420 MeV in the $\pi f_0(980)$ invariant mass. We find a narrow peak in the $\pi^+\pi^-$ invariant mass distribution, which originates from the $f_0(980)$ amplitude. Similarly, we also study the triangle mechanism for the decay $\tau \to \nu \pi^- a_0(980)$, with the $a_0(980)$ decaying into $\pi^0\eta$. The formalism leads to final branching ratios for $\pi^- f_0(980)$ and $\pi^- a_0(980)$ of the order of 4×10^{-4} and 7×10^{-5}, respectively, which are within present measurable range. Experimental verification of these predictions will shed light on the nature of the scalar mesons and on the origin of the "$a_1(1420)$" peak observed in other reactions.

DOI: 10.1103/PhysRevD.99.016021

I. INTRODUCTION

Triangle singularities were studied in detail by Landau [1], and they emerge from a process symbolized by a triangle Feynman diagram in which one particle A decays into 1 and 2, 2 decays into $B + 3$, and $1 + 3$ merge to give another state C or simply rescatter. Under certain conditions where all particles 1,2,3 can be placed on shell, 1 and B are antiparallel and the process can occur at the classical level [2] (Coleman Norton Theorem), the process develops a singularity visible in a peak in the corresponding cross sections. While no clear such physical processes were observed for a long time, the situation reverted recently where clear cases have been observed and many reactions have been suggested to show such phenomena. A particular case is the triangle singularity studied in [3–5] where a peak seen by the COMPASS Collaboration in the $\pi f_0(980)$ final state [6], branded originally as a new resonance, "$a_1(1420)$," was naturally explained in terms of the triangle singularity stemming from the original production of $K^* \bar{K}$, decay of K^* into πK, and fusion of $K\bar{K}$ to give the $f_0(980)$ resonance.

*dailr@lnnu.edu.cn
†yuqx@mail.bnu.edu.cn
‡oset@ific.uv.es

The interest in triangle singularities has grown recently. In addition to the interpretation of the "$a_1(1420)$" as a triangle singularity, the $f_1(1420)$, officially in the PDG tables [7], was also shown to correspond to the "$f_1(1285)$" decay into $K^* \bar{K}$, with the "$\pi a_0(980)$ decay width" [8] also corresponding to the "$f_1(1285)$" [9]. Similarly, the "$f_2(1810)$" was also shown to come from a triangle singularity [10]. Some particular reactions have also been studied and partial contributions or peaks in the cross sections have also been associated with triangle singularities, and suggestions of new reactions to see them have been proposed [11–29].

The issue of triangle singularities got a revival when it was suggested that the narrow signal at 4450 MeV observed by the LHCb Collaboration and branded as a pentaquark state, $P_c(4450)$ [30], could be due to a triangle singularity [31–33]. Concretely, in [33], the mechanism is assumed to be $\Lambda_b \to \Lambda^* \chi_{c_1}$, followed by $\Lambda^* \to KN$ and $\chi_{c_1} N \to J/\psi p$ (N, p and Λ^* stand for nucleon, proton, and excited Λ state, respectively), but it was shown in [34] that with the experimentally preferred quantum numbers of the $P_c(4450)$ this mechanism requires the scattering $\chi_{c_1} p \to J/\psi p$ at threshold, demanding p-wave or d-wave, which vanishes, and thus cannot be the explanation for the experimental peak.

In the present work, we study the reactions $\tau^- \to \nu_\tau \pi^- f_0(980)$ and $\tau^- \to \nu_\tau \pi^- a_0(980)$. The original τ^- decays into a ν_τ and a $d\bar{u}$ state that has $I_3 = -1$, $I = 1$. The further hadronization including a $\bar{q}q$ pair forms two mesons conserving isospin. Hence, both decays modes are allowed. Since $f_0(980)$, $a_0(980)$ couple mostly to $K\bar{K}$, the reaction favors the formation of this pair, in addition to the π^-. Hence it proceeds via $K^*\bar{K}$ production, followed by K^* decay to $\pi^- K$ and the $K\bar{K}$ fuse to produce the $f_0(980)$ or the $a_0(980)$. Then we have a triangle mechanism that could or not produce a singularity. However we show that it develops a triangle singularity at an invariant mass $M_{\rm inv}(\pi R)(R \equiv f_0, a_0) \simeq 1420$ MeV. Interestingly, the triangle mechanism that produces a peak in this invariant mass distribution is the same one that produced the "$a_1(1420)$" peak observed in the COMPASS experiment.

One should note that in $\tau^- \to \nu_\tau \pi^- f_0(980)$, after the decay of $f_0(980)$ into $\pi^+\pi^-$ we have the final product $\nu_\tau\pi^-\pi^+\pi^-$. This reaction has been measured experimentally [35–40], and the main feature is a dominance of $a_1(1260)$ production which decays into $\pi\rho$. This decay mode is also very important, with a branching ratio of about 10^{-1}. This is interesting to mention because the branching ratios that we get for our reactions are of the order of 10^{-4}. They have not been yet measured, but there is a related reaction $\tau^- \to \nu_\tau\pi^- f_1(1285)$ which has been measured, with a branching ratio 3.9×10^{-4}. The good thing for the proposed reaction is that it peaks mostly around $M_{\rm inv}(\pi^-\pi^+\pi^-) \sim 1420$ MeV, which is at the tail of the $a_1(1260)$,[1] and hence by looking in detail in this region one gets rid of the bulk of the $\nu_\tau\pi^-\pi^+\pi^-$ strength. For the $\tau^- \to \nu_\tau\pi^-\pi^0\eta$ there are also experiments performed [41–43]. Once again, the $\pi^0\eta$ invariant mass distribution around the $a_0(980)$ with $M_{\rm inv}(\pi^-\pi^0\eta)$ around 1420 MeV has not been explicitly measured and we hope the present work encourages future experiments looking in detail into this region.

The theoretical works on the $\tau^- \to \nu_\tau\pi^-\pi^+\pi^-$ are also extense [44–50], and the $\tau^- \to \nu_\tau\pi^-\pi^0\eta$ has also got attention in [51,52]. Some recent reviews on these issues can be seen in [53,54]. There is a consensus on the relevance of the $a_1(1260)$ production in all these works, which is visible in the $M_{\rm inv}(\pi^-\pi^+\pi^-)$ distribution, and its decay to $\pi\rho$, where ρ is also visible in the $M_{\rm inv}(\pi^-\pi^+)$ distribution, with some smaller contribution from the $\sigma(f_0(500))$. A detailed study of the reaction, paying special attention to analyticity and three body unitarity, has been done in [55], which allows to obtain the $a_1(1260)$ pole in the complex plane.

However, the channel that we study $\tau^- \to \nu_\tau\pi^- f_0(980)$ is a very particular channel, which is unrelated to the dynamics used in the former works to study the main decay channel in $\nu_\tau\pi^-\pi^+\pi^-$ ($\tau^- \to \nu_\tau\pi^-\pi^0\eta$). As we shall see, given the fact that the $f_0(980)$ couples mostly to $K\bar{K}$ (and so does the $a_0(980)$) and the fact that these resonances are dynamically generated from the meson interaction, we must rely upon a mechanism where $K\bar{K}$ has to be produced. If in addition we want to have an extra pion this calls for $K\bar{K}\pi$ production, and the $K\pi$ will be dominated by K^*, such that $K^*\bar{K}$ production is at the root of the $\pi^- f_0(\pi^- a_0)$ production. This dynamics is quite different from the one applied in former theoretical papers to explain the bulk of the $\tau^- \to \nu_\tau\pi^-\pi^+\pi^-$ reaction.

The other issue present in this reaction is the G-parity. Its relevance in τ^- decays was put forward in Ref. [56]. The $\pi^- f_0(980)$ and $\pi^- a_0(980)$ have negative and positive G-parity, respectively. The formalism has to provide the means to filter the states of G-parity just after the weak decay, from the operators involved in the $Wd\bar{u}$ vertex. Fortunately a formalism has been developed recently [57,58] in which the G-parity appears explicitly in the amplitudes written at the macroscopic meson level after the hadronization to produce two mesons. By means of this formalism, we can easily evaluate the loops involved in the triangle mechanism and predict quantitative mass distributions for the τ^- decay in these modes. This is made possible because the radial matrix elements of the quark wave functions, which are a source of large uncertainties and we do not explicitly evaluate, are implicitly taken into account by making use of the experimental value of the $\tau \to \nu_\tau K^{*0}K^-$ branching ratio, which is the first step in our loop mechanism.

By means of this approach, we obtain $\frac{d^2\Gamma}{dM_{\rm inv}(\pi^- R)dM_{\rm inv}(\pi^+\pi^-)}$ or $\frac{d^2\Gamma}{dM_{\rm inv}(\pi^- R)dM_{\rm inv}(\pi^0\eta)}$ which show the shapes of the $f_0(980)$ and $a_0(980)$ resonances in the $\pi^+\pi^-$ or $\pi^0\eta$ mass distributions, respectively. Then we integrate over the $\pi^+\pi^-$ or $\pi^0\eta$ invariant masses and obtain $\frac{d^2\Gamma}{dM_{\rm inv}(\pi^- R)}$, which shows a clear peak around $M_{\rm inv}(\pi^- R) \simeq 1420$ MeV. The further integration over $M_{\rm inv}(\pi^- R)$ provides us branching ratios for $\tau^- \to \nu_\tau\pi^- f_0(980)$ and $\tau^- \to \nu_\tau\pi^- a_0(980)$ production, and we obtain values of 4×10^{-4} and 7×10^{-5} for these two ratios, respectively, which are well within measurable range.

The measurement of such reactions and comparison with the present results should be very useful since it conjugates several interesting issues:

(i) It provides one more measurable example of a triangle singularity, which have been quite sparse up to now.

(ii) It serves as a further test of the nature of the $f_0(980)$ and $a_0(980)$, since they are not directly produced from the weak decay, but come from fusion of $K\bar{K}$ in a scattering process, establishing a link with the chiral unitary approach to these resonances where they are shown not to correspond to $q\bar{q}$ state but are generated by the scattering of pseudoscalar mesons in coupled channels.

(iii) The filters of the G-parity in the amplitudes can also provide information that can be extrapolated to $\tau^- \to \nu_\tau M_1 M_2$ decays with $M_1 M_2$ pairs of states that have a given G-parity as $\pi\rho$, $\pi\omega$, $\eta\rho$ and $\eta'\rho$.

[1] See Fig. 1 of Ref. [40] where it is shown that the strength of $\pi\pi\pi$ mass distribution in that region is 5–6 times smaller than that at the peak.

With the possible advent of future τ^- facilities,[2] predictions like the present one and the motivation given, should provide the grounds for proposals at that machine. Yet, other existing facilities have also access to these reactions since rates of 10^{-5} and smaller are common in τ^- decays [7].

A reaction close to the present one is the $\tau^- \to \nu_\tau \pi^- f_1(1285)$. The reaction has been measured [7] with a branching ratio $(3.9 \pm 0.5) \times 10^{-4}$. In [62], a mechanism similar to the present one is presented in which $K^*\bar{K}$ in an intermediate state merge to produce the $f_1(1285)$, also dynamically generated from the $K^*\bar{K}$ interaction [63,64]. In this case, a triangle singularity appearing around 1800 MeV in the $\pi^- f_1(1285)$ invariant mass only shows up at the end of the phase space, such that no visible peak associated to this triangle singularity is seen in the mass distribution and other interpretations are possible [65]. In the present case, we shall see that the peak in the $\pi^- f_0(a_0)$ mass distributions is very strong and clear.

II. FORMALISM

We will study the effect of triangle singularities in the decay of $\tau^- \to \nu_\tau \pi^- \pi^+ \pi^-$ and $\tau^- \to \nu_\tau \pi^- \pi^0 \eta$ decays with $\pi^+\pi^-$ forming the $f_0(980)$ and $\pi^0\eta$ the $a_0(980)$. The complete Feynman diagrams for the decay with the triangle mechanism through the $f_0(980)$ and $a_0(980)$ are shown in Figs. 1 and 2.

In Fig. 1, we investigate the $\tau^- \to \nu_\tau \pi^- \pi^+ \pi^-$ decay via $f_0(980)$ formation, where Fig. 1(a) shows the process $\tau^- \to \nu_\tau K^{*0} K^-$ followed by the K^{*0} decay into $\pi^- K^+$ and the merging of the $K^- K^+$ into $f_0(980)$, and Fig. 1(b) shows the process $\tau^- \to \nu_\tau K^{*-} K^0$ followed by the $\bar{K}^{*0}$ decay into $\pi^- \bar{K}^0$ and the merging of the $K^0 \bar{K}^0$ into $f_0(980)$. Each process generates a singularity, and we will see a signal for the isospin $I = 0$ resonance state $f_0(980)$ formation in the invariant mass of $\pi^+\pi^-$. In the study of Refs. [66–71], the $f_0(980)$ appears as the dynamically generated state from the $\pi^+\pi^+$, $\pi^0\pi^0$, K^+K^-, $K^0\bar{K}^0$, and $\eta\eta$ in the coupled-channels calculation.

Similarly, in Fig. 2, we investigate the $\tau^- \to \nu_\tau \pi^- \pi^0 \eta$ decay via $a_0(980)$ formation, where Fig. 2(a) shows the process $\tau^- \to \nu_\tau K^{*0} K^-$ followed by the K^{*0} decay into $\pi^- K^+$ and the merging of the $K^- K^+$ into $a_0(980)$, and the process $\tau^- \to \nu_\tau K^{*-} K^0$ followed by the K^{*-} decay into $\pi^- \bar{K}^0$ and the merging of the $K^0 \bar{K}^0$ into $a_0(980)$. Both processes also generate a singularity, and we will see a signal for the isospin $I = 1$ resonance state $a_0(980)$ in the invariant mass of $\pi^0\eta$. In the study of Refs. [66–71], the $a_0(980)$ appears as the dynamically generated state of K^+K^-, $K^0\bar{K}^0$, and $\pi^0\eta$ in the coupled-channels calculation. The momenta assignment for the decay process is given in Fig. 1(a).

Let us address, next, the evaluation of the $\tau \to \nu_\tau K^{*0} K^-$, $\nu_\tau K^{*-} K^0$ parts. The production is assumed to proceed first from the Cabibbo favored $\bar{u}d$ production from the W^- which then hadronizes producing an $s\bar{s}$ with quantum numbers of the vacuum, which are implemented with the $^3P_0$ model [72–74]. This leads to the $K^{*0}K^-$ and K^0K^{*-} states with the same weight. In Refs. [57,58], the mechanism for hadronization is done in detail. The first step corresponds to the flavor combinations in the hadronization. There it is shown that $d(\bar{s}s)\bar{u} = (d\bar{s})s\bar{u}$ gives rise to K^0K^{*-} and $K^{*0}K^-$ with the same weight (see Eqs. (2) and (3) of Ref. [57]). The second step corresponds to the detailed study of the spin-angular momentum algebra to combine the quarks for the $^3P_0$ $\bar{s}s$ state ($L' = 1$, $S' = 1$, $J' = 0$) with a $\bar{d}$ quark in $L = 1$ to have finally s-wave production of the two mesons. In Ref. [57], the p-wave vector-pseudoscalar production was ruled out based on the theoretical results, and experimental results that show the vector-pseudoscalar pairs coupling to an axial vector resonance $J^{PC} = 1^{++}$ [75], which proceeds with s-wave. The needed results from [57,58] are given in the next subsection.

A. $\tau \to \nu_\tau K^{*0} K^-$ decay

The elementary quark interaction is given by

$$H = \mathcal{C} L^\mu Q_\mu, \tag{1}$$

where $\mathcal{C}$ contains the couplings of the weak interaction. The leptonic current is given by

$$L^\mu = \langle \bar{u}_\nu | \gamma^\mu - \gamma^\mu \gamma_5 | u_\tau \rangle, \tag{2}$$

and the quark current by

$$Q^\mu = \langle \bar{u}_d | \gamma^\mu - \gamma^\mu \gamma_5 | v_{\bar{u}} \rangle. \tag{3}$$

As is usual in the evaluation of decay widths to three final particles, it is convenient to evaluate the phase space in a frame where two final particles are at rest. We choose the frame where the two mesons system is at rest. For the evaluation of the matrix element Q_μ we assume that the quark spinors are at rest in that frame [57,58], then we have $\gamma^0 \to 1$, $\gamma^i\gamma_5 \to \sigma^i$ in terms of bispinors χ and after the spin angular momentum combination we have

$$\begin{aligned} Q_0 &= \langle \chi' | 1 | \chi \rangle \to M_0, \\ Q_i &= \langle \chi' | \sigma_i | \chi \rangle \to N_i. \end{aligned} \tag{4}$$

Denoting for simplicity,

[2] Projects exist, one of them at Hefei, China [59], another one at Novosibirsk [60], and the Belle II update [61] (X. G. He, private communication).

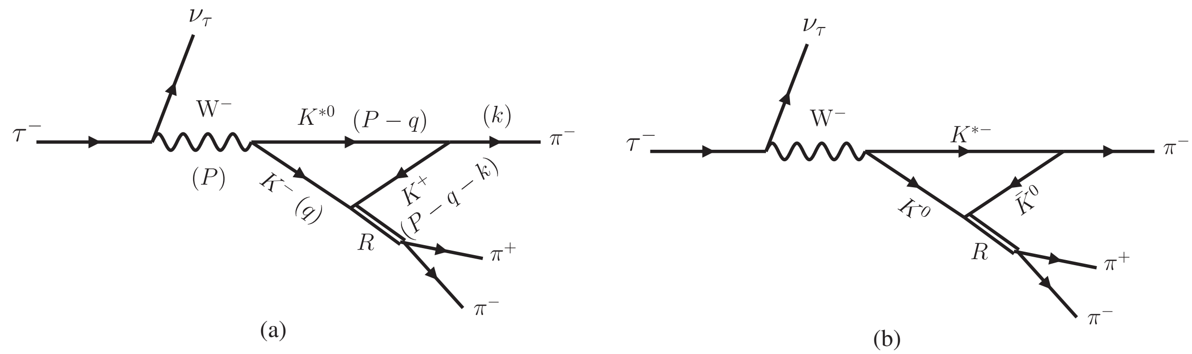

FIG. 1. Diagram for the decay of $\tau^- \to \nu_\tau \pi^- \pi^+ \pi^-$. (a) The process $\tau^- \to \nu_\tau K^{*0} K^-$ followed by the K^{*0} decay into $\pi^- K^+$ and the merging of the $K^- K^+$ into $f_0(980)$; (b) The process $\tau^- \to \nu_\tau K^{*-} K^0$ followed by the K^{*-} decay into $\pi^- \bar{K}^0$ and the merging of the $K^0 \bar{K}^0$ into $f_0(980)$. The double line, labeled R, indicates that we are taking the $K\bar{K} \to \pi^+\pi^-$ scattering amplitudes. The brackets in figure (a) indicate the momenta of the particles.

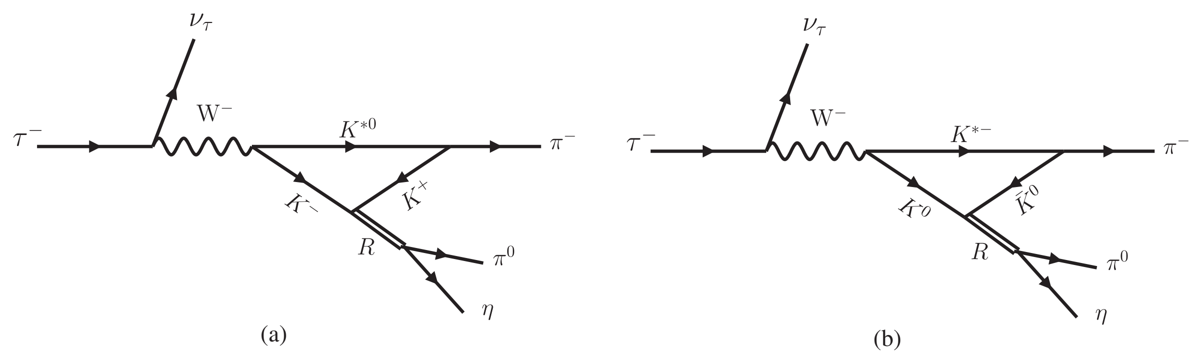

FIG. 2. Diagram for the decay of $\tau^- \to \nu_\tau \pi^- \pi^0 \eta$. (a) The process $\tau^- \to \nu_\tau K^{*0} K^-$ followed by the K^{*0} decay into $\pi^- K^+$ and the merging of the $K^- K^+$ into $a_0(980)$; (b) The process $\tau^- \to \nu_\tau K^{*-} K^0$ followed by the K^{*-} decay into $\pi^- \bar{K}^0$ and the merging of the $K^0 \bar{K}^0$ into $a_0(980)$. The double line, labeled R, indicates that we are taking the $K\bar{K} \to \pi^0 \eta$ scattering amplitudes.

$$\overline{L}^{\mu\nu} = \overline{\sum}\sum L^\mu L^{\nu\dagger}, \tag{5}$$

to obtain the τ width we must evaluate

$$\begin{aligned}\overline{\sum}\sum |t|^2 &= \overline{\sum}\sum L^\mu L^{\nu\dagger} Q_\mu Q_\nu^*, \\ &= \bar{L}^{00} M_0 M_0^* + \bar{L}^{0i} M_0 N_i^* + \bar{L}^{i0} N_i M_0^* + \bar{L}^{ij} N_i N_j^*,\end{aligned} \tag{6}$$

with $\bar{L}^{\mu\nu}$ given by

$$\begin{aligned}&\overline{\sum}\sum L^\mu L^{\nu\dagger} \\ &= \frac{1}{m_\nu m_\tau} (p'^\mu p^\nu + p'^\nu p^\mu - g^{\mu\nu} p' \cdot p + i\epsilon^{\alpha\mu\beta\nu} p'_\alpha p_\beta),\end{aligned} \tag{7}$$

where p, p' are the momenta of the τ and ν_τ, respectively, and we use the field normalization for fermions of Ref. [76].

From the work [57,58] we obtain the results for the $J = 1$, $J' = 0$ case, which correspond to the $\tau \to \nu_\tau K^{*0} K^-$ decay.

$$\begin{aligned}M_0 &= \frac{1}{\sqrt{6}} \frac{1}{4\pi}, \quad \text{for any } M, \\ N_\mu &= (-1)^{-\mu} \frac{1}{\sqrt{3}} \frac{1}{4\pi} \mathcal{C}(111; M, -\mu, M-\mu),\end{aligned} \tag{8}$$

where M is the third component of J and μ is the index of N_i in spherical basis, with $\mathcal{C}(\cdots)$ a Clebsch-Gordan coefficient.

It was shown in [57,58] that the order in which the vector and pseudoscalar mesons are produced is essential to understand the G-parity symmetry of these reactions. Then from [57,58] we write here the results for PV production $J = 0$, $J' = 1$, which correspond to the $\tau \to \nu_\tau K^0 K^{*-}$ decay,

$$\begin{aligned}M_0 &= \frac{1}{\sqrt{6}} \frac{1}{4\pi}, \quad \text{for any } M', \\ N_\mu &= -(-1)^{-\mu} \frac{1}{\sqrt{3}} \frac{1}{4\pi} \mathcal{C}(111; M', -\mu, M'-\mu).\end{aligned} \tag{9}$$

Note that while M_0 is the same for VP and PV productions, N_i changes sign for VP and PV. This sign is essential for the conservation of G-parity in the reaction, as we shall see. Indeed, at the quark level the primary $d\bar{u}$ state produced has $I_3 = -1$ and hence $I = 1$. The G-parity of a $q\bar{q}$ pair is given by $(-1)^{L+S+I}$. As we mentioned $L = 1$, $I = 1$ and the spin of the state is 0 for the 1 operator and 1 for the σ^i operator of Eq. (4). This means that the term M_0 proceeds with positive G-parity, while N_i has negative G-parity. Since π, $f_0(980)$, and $a_0(980)$ have G-parity $-, +, -$, respectively, then $\pi^- f_0(980)$ will proceed with the N_i amplitude, while $\pi^- a_0(980)$ proceeds with the M_0 term and there is no simultaneous contribution of the two terms in these reactions. This we shall see analytically when evaluating explicitly the amplitudes for the processes of Figs. 1 and 2.

As seen in Eq. (1), we have the unknown constant $\mathcal{C}$ in our approach which includes factors involving the matrix elements of the radial quark wave functions (the spin-angular momentum variables are explicitly accounted for in the work of [57,58]). We then determine $\mathcal{C}$ from the experimental ratio of $\tau \to \nu_\tau K^{*0} K^-$. For this we use the results of [57,58] for this reaction.

By taking the quantization axis along the direction of the neutrino in the τ^- rest frame, we find

$$\bar{\sum} \sum |t|^2 = \frac{\mathcal{C}^2}{m_\tau m_\nu} \left(\frac{1}{4\pi}\right)^2 \times \left[(E_\tau E_\nu + p^2) \frac{1}{2} h_i^2 + \left(E_\tau E_\nu - \frac{1}{3} p^2\right) \bar{h}_i^2 \right] = \frac{\mathcal{C}^2}{m_\tau m_\nu} \left(\frac{1}{4\pi}\right)^2 \left(\frac{3}{2} E_\tau E_\nu + \frac{1}{6} p^2\right) \quad (10)$$

where $h_i = \bar{h}_i = 1$, p is the momentum of the τ, or ν_τ, in the $K^{*0} K^-$ rest frame, given by

$$p = p_\nu = p_\tau = \frac{\lambda^{1/2}(m_\tau^2, m_\nu^2, M_{\mathrm{inv}}^2(K^{*0} K^-))}{2 M_{\mathrm{inv}}(K^{*0} K^-)}, \quad (11)$$

and $E_\nu = p$, $E_\tau = \sqrt{m_\tau^2 + p^2}$.

Now for $\tau \to \nu_\tau K^{*0} K^-$ decay, we obtain

$$\frac{d\Gamma}{dM_{\mathrm{inv}}(K^{*0} K^-)} = \frac{2 m_\tau 2 m_\nu}{(2\pi)^3} \frac{1}{4 m_\tau^2} p'_\nu \tilde{p}_K \bar{\sum} \sum |t|^2, \quad (12)$$

where p'_ν is the neutrino momentum in the τ rest frame

$$p'_\nu = \frac{\lambda^{1/2}(m_\tau^2, m_\nu^2, M_{\mathrm{inv}}^2(K^{*0} K^-))}{2 m_\tau}, \quad (13)$$

and $\tilde{p}_K$ the momentum of K^- in the $K^{*0} K^-$ rest frame given by

$$\tilde{p}_K = \frac{\lambda^{1/2}(M_{\mathrm{inv}}^2(K^{*0} K^-), m_{K^{*0}}^2, m_{K^-}^2)}{2 M_{\mathrm{inv}}(K^{*0} K^-)}. \quad (14)$$

Experimentally, the branching ratio of $\mathcal{B}(\tau \to \nu_\tau K^{*0} K^-)$ decay,

$$\mathcal{B}(\tau \to \nu_\tau K^{*0} K^-) = \frac{1}{\Gamma_\tau} \Gamma(\tau \to \nu_\tau K^{*0} K^-) = (2.1 \pm 0.4) \times 10^{-3}, \quad (15)$$

and then

$$\frac{\mathcal{C}^2}{\Gamma_\tau} = \frac{\mathcal{B}(\tau \to \nu_\tau K^{*0} K^-)}{\int_{m_{K^-} + m_{K^{*0}}}^{m_\tau} \frac{1}{(2\pi)^3} \frac{1}{m_\tau^2} p'_\nu \tilde{p}_K \frac{1}{(4\pi)^2} \left(\frac{3}{2} E_\tau E_\nu + \frac{1}{6} p^2\right) dM_{\mathrm{inv}}(K^{*0} K^-)}, \quad (16)$$

from which we can evaluate the value of the constant $\frac{\mathcal{C}^2}{\Gamma_\tau}$. We obtain $\frac{\mathcal{C}^2}{\Gamma_\tau} = (2.10 \pm 0.40) \times 10^{-5}\ \mathrm{MeV}^{-3}$, where the errors come from the uncertainty of $\mathcal{B}(\tau \to \nu_\tau K^{*0} K^-)$.

In the evaluation of Eq. (16), we have considered K^{*0} as an elementary particle, while it should be taken into account that it has a mass distribution since it decays to πK. The proper way to do this is to fold the $\Gamma(\tau \to \nu_\tau K^{*0} K^-)$ width with the spectral function (mass distribution) of the K^{*0}. This is done explicitly in [57,58], and we have also done it here. We find that the difference between these two calculations is 4%, which is much smaller than the uncertainty that we have at the end from other sources. Due to this, we stick to the simple elementary particle formulation for the K^*.

It should be interesting to compare the $K^{*0} K^-$ mass distribution of Eq. (12) with experiment. However, this observable is not available. There are invariant mass distributions for $K^+ \pi^- K^-$ in $\tau^- \to \nu_\tau K^+ \pi^- K^-$ (see Fig. 1 of Ref. [77] and Fig. 7 of Ref. [39]) but they contain other contributions than $K^{*0} K^-$. However, according to Ref. [77] the $K^+ \pi^- K^-$ spectrum is dominated by $K^{*0} K^-$. The $\tau^- \to \nu_\tau K^+ \pi^- K^-$ has also received much attention theoretically related to issues of neutrino masses, the determination of α_s, and the contribution of the vector and axial vector currents, which is still under debate [78–81]. Yet, the $\tau^- \to \nu_\tau K^{*0} K^-$ part of it has not been isolated in these studies. For the present work we do not need to enter this discussion, it is sufficient to show that the $K^{*0} K^-$ mass distribution is in a reasonable agreement with data. Since this comparison is not possible at the present time, we mention in support of our picture the mass of distribution of ηK^{*-} in the $\tau^- \to \nu_\tau \eta K^{*-}$ decay, see Fig. 3,

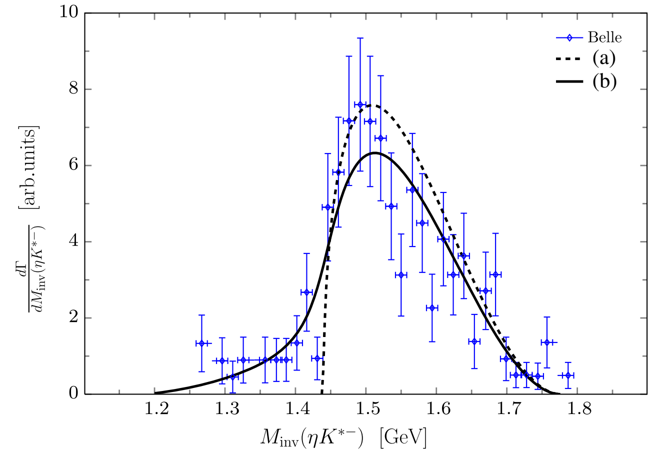

FIG. 3. The mass distribution of ηK^{*-} in $\tau^- \to \nu_\tau \eta K^{*-}$ decay. (a) in this figure stands for the situation when the mass of K^{*-} is fixed, while (b) stands for convoluting the $M_{\rm inv}$ distribution with the K^{*-} spectral function to account for its mass distribution.

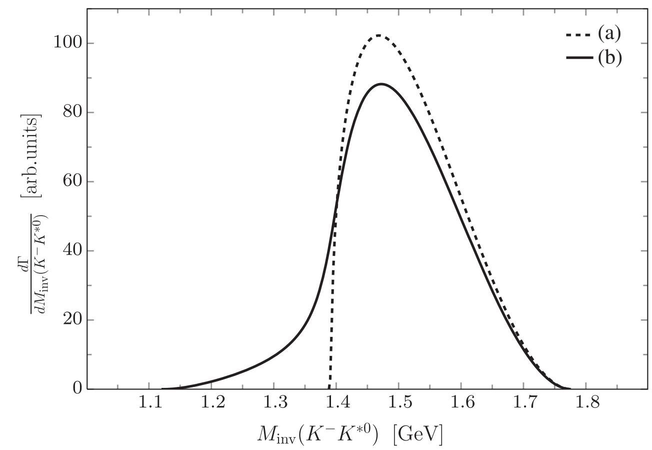

FIG. 4. The mass distribution of $K^- K^{*0}$ in $\tau^- \to \nu_\tau K^- K^{*0}$ decay. (a) in this figure stands for the situation when the mass of K^{*0} is fixed, while (b) stands for convoluting the $M_{\rm inv}$ distribution with the K^{*0} spectral function to account for its mass distribution.

which is in remarkable agreement with experiment. With the necessary caveat, it is also interesting to see what we obtain for the $K^{*0}K^-$ mass distribution with the present formalism [57]. We show this in Fig. 4.

We refrain from plotting data in Fig. 4 since they contains $K^-K^+\pi^-$ events from all sources. Yet, assuming, as in Ref. [77], that the $K^-K^+\pi^-$ distribution is dominated by $K^{*0}K^-$, the agreement of Fig. 4 with the data of Refs. [39,77] is very good.

B. Evaluation of the triangle diagram

The first thing that we should note is that in Figs. 1 and 2 the double line R stands for $f_0(980)$ or $a_0(980)$ scattering amplitudes. In the actual calculation, we explicitly use the $K\bar{K} \to \pi^+\pi^-(\pi^0\eta)$ amplitudes, calculated in the chiral unitary approach [66,69,70]. These amplitudes depend only on the $\pi^+\pi^-(\pi^0\eta)$ invariant mass, which is an external variable that does not change in the loop integration, and can be factorized outside the loop integral. The $K^* \to K\pi$ vertex is obtained from the VPP Lagrangian

$$\mathcal{L}_{VPP} = -ig\langle V^\mu [P, \partial_\mu P]\rangle, \tag{17}$$

and the brackets $\langle \ldots \rangle$ mean the trace over the SU(3) flavour matrices, with the coupling g given by $g = m_V/2f_\pi$ in the local hidden gauge approach, with $m_V = 800$ MeV and $f_\pi = 93$ MeV. Equation (17) is rather general and can be obtained as well in massive Yang-Mills theory [82–85]. From Eq. (17), the vertex $K^* \to K\pi$ is of the type $\epsilon[k - (-q-k)]$.

The loop function in Fig. 1(a) is then given by

$$t'^{\mu}_L \equiv i\int \frac{d^4q}{(2\pi)^4} \frac{1}{(P-q)^2 - m^2_{K^*} + i\epsilon} \frac{1}{q^2 - m^2_{K^-} + i\epsilon} \times \frac{1}{(P-q-k)^2 - m^2_K + i\epsilon} \epsilon^\mu g \epsilon[k - (-q-k)]. \tag{18}$$

It is convenient to evaluate this expression in the rest frame of the final three mesons. The reason is that in this frame, and for the triangle singularity energy, the intermediate K^* is on shell and with very slow momentum, such that its ϵ^0 component can be neglected, simplifying the formalism. We shall come back to this point and evaluate the uncertainty of this approximation. After this, we perform analytically the q^0 integration and we obtain a remaining integral in d^3q [34,86] and we obtain

$$t'^{i}_L = \int \frac{d^3q}{(2\pi)^3} \frac{1}{8\omega_{K^*}\omega_{K^+}\omega_{K^-}} \frac{1}{k^0 - \omega_{K^+} - \omega_{K^*} + i\frac{\Gamma_{K^*}}{2}} \boldsymbol{\epsilon}_i g \boldsymbol{\epsilon}_j (2\boldsymbol{k} + \boldsymbol{q})_j \frac{1}{P^0 + \omega_{K^-} + \omega_{K^+} - k^0} \frac{1}{P^0 - \omega_{K^-} - \omega_{K^+} - k^0 + i\epsilon} \times \frac{2P^0\omega_{K^-} + 2k^0\omega_{K^+} - 2(\omega_{K^-} + \omega_{K^+})(\omega_{K^-} + \omega_{K^+} + \omega_{K^*})}{P^0 - \omega_{K^*} - \omega_{K^-} + i\frac{\Gamma_{K^*}}{2}}, \tag{19}$$

with $P^0 = M_{\rm inv}(\pi^- f_0)$, $\omega_{K^-} = \sqrt{\boldsymbol{q}^2 + m_K^2}$, $\omega_{K^+} = \sqrt{(\boldsymbol{q}+\boldsymbol{k})^2 + m_K^2}$, and $\omega_{K^*} = \sqrt{\boldsymbol{q}^2 + m_{K^*}^2}$

$$k^0 = \frac{M_{\rm inv}^2(\pi^- f_0) + m_\pi^2 - M_{\rm inv}^2(\pi^+\pi^-)}{2M_{\rm inv}(\pi^- f_0)}, \tag{20}$$

$$k = \frac{\lambda^{1/2}(M_{\rm inv}^2(\pi^- f_0), m_\pi^2, M_{\rm inv}^2(\pi^+\pi^-))}{2M_{\rm inv}(\pi^- f_0)}. \tag{21}$$

Similarly, we can get the triangle amplitude for the $\pi^- a_0$ case. Note also that an $i\epsilon$ in the propagators involving ω_{K^*} is replaced by $i\frac{\Gamma_{K^*}}{2}$.

The next step is to realize that in Eq. (19) the only vector remaining after the d^3q integration is $\boldsymbol{k}$ and hence the result of $\int d^3q\boldsymbol{q}\cdots$ integration will be proportional to $\boldsymbol{k}$. Thus,

$$\int d^3q f(\boldsymbol{k},\boldsymbol{q}) q^i = A k^i, \qquad A = \int d^3q f(\boldsymbol{k},\boldsymbol{q}) \frac{\boldsymbol{q}\cdot\boldsymbol{k}}{|\boldsymbol{k}|^2}, \tag{22}$$

where $f(\boldsymbol{k},\boldsymbol{q})$ is the function in the integrand of Eq. (19) when we remove $\boldsymbol{\epsilon_i} g \boldsymbol{\epsilon_j}(2\boldsymbol{k}+\boldsymbol{q})_j$. Hence, $\boldsymbol{q}$ in $2\boldsymbol{k}+\boldsymbol{q}$ in Eq. (19) can be replaced effectively by $\frac{\boldsymbol{q}\cdot\boldsymbol{k}}{|\boldsymbol{k}|^2}\boldsymbol{k}$. Equation (19) can now be simplified replacing $(2\boldsymbol{k}+\boldsymbol{q})$ by $\boldsymbol{k}(2+\frac{\boldsymbol{q}\cdot\boldsymbol{k}}{|\boldsymbol{k}|^2})$.

In Eq. (8), we need M, the third component of J. In order to evaluate the loops of Figs. 1 and 2, we find most convenient to take the z direction along the momentum $\boldsymbol{k}$ of the pion produced (see Fig. 1(a)), since we found the amplitude is proportional to $\boldsymbol{\epsilon}\cdot\boldsymbol{k}$. If the z direction is chosen along $\boldsymbol{k}$, in the $\boldsymbol{\epsilon}\cdot\boldsymbol{k}$ factor only the $\boldsymbol{\epsilon}_z$ component ($\boldsymbol{\epsilon}_0$ in spherical basis) is operative and $\boldsymbol{\epsilon}\cdot\boldsymbol{k} = |\boldsymbol{k}| = k$. This also means that only $M=0$ contributes in the loop and this allows us to calculate trivially the M_0, N_μ amplitude in that frame. Indeed, for $J=1$, $J'=0$,

$$M_0 \to \frac{1}{\sqrt{6}}\frac{1}{4\pi}, \qquad N_\mu \to (-1)^{-\mu}\frac{1}{\sqrt{3}}\frac{1}{4\pi}\mathcal{C}(111;0,-\mu,-\mu), \tag{23}$$

and for $J=0$, $J'=1$, M_0 is the same and N_μ changes sign.

Explicit calculation of the Clebsch-Gordan coefficients in Eq. (23) gives

$$N_{\mu=+1} = -\frac{1}{\sqrt{3}}\frac{1}{4\pi}\frac{1}{\sqrt{2}}, \qquad N_{\mu=-1} = \frac{1}{\sqrt{3}}\frac{1}{4\pi}\frac{1}{\sqrt{2}}, \qquad N_{\mu=0} = 0, \tag{24}$$

which in cartesian coordinate can be written as

$$N_i = \frac{1}{\sqrt{3}}\frac{1}{4\pi}\delta_{i1}, \tag{25}$$

the index 1 for the x direction. Since only the $M=0$ component of the polarization contributes, we omit the explicit $\boldsymbol{\epsilon_i} g \boldsymbol{\epsilon_j}$ factor in Eq. (19) and define the t_L such that

$$t_L = \int \frac{d^3q}{(2\pi)^3}\frac{1}{8\omega_{K^*}\omega_{K^+}\omega_{K^-}}\frac{1}{k^0-\omega_{K^+}-\omega_{K^*}+i\frac{\Gamma_{K^*}}{2}}\left(2+\frac{\boldsymbol{q}\cdot\boldsymbol{k}}{|\boldsymbol{k}|^2}\right)\frac{1}{P^0+\omega_{K^-}+\omega_{K^+}-k^0}\frac{1}{P^0-\omega_{K^-}-\omega_{K^+}-k^0+i\epsilon}$$
$$\times\frac{2P^0\omega_{K^-}+2k^0\omega_{K^+}-2(\omega_{K^-}+\omega_{K^+})(\omega_{K^-}+\omega_{K^+}+\omega_{K^*})}{P^0-\omega_{K^*}-\omega_{K^-}+i\frac{\Gamma_{K^*}}{2}}\theta(q_{\rm max}-q^*), \tag{26}$$

where we include the regulator $\theta(q_{\rm max}-q^*)$.

Equation (26) is already convergent. However, when evaluating the $K\bar{K}\to\pi\pi$, $K\bar{K}\to\pi\eta$ amplitudes in the chiral unitary approach to get the $f_0(980)$ or $a_0(980)$ resonances, a cutoff, $q_{\rm max}$, in the $\boldsymbol{q}$ variable in the meson-meson loop function is used. Then, it is found in Ref. [87] that the approach is equivalent to solving the Bethe-Salpeter equation with a potential of the type $V\theta(q_{\rm max}-|\boldsymbol{q}'|)\theta(q_{\rm max}-|\boldsymbol{q}|)$ and this structure is transferred to the scattering amplitude that becomes $t\theta(q_{\rm max}-|\boldsymbol{q}'|)\theta(q_{\rm max}-|\boldsymbol{q}|)$, with $\boldsymbol{q}$, $\boldsymbol{q}'$ the incoming and outgoing meson momenta in the $K\bar{K}$ rest frame. Accordingly, when we use the $K\bar{K}\to\pi\pi$, $K\bar{K}\to\pi\eta$ scattering amplitudes, we implement these cutoff factors, with $q_{\rm max} = 600$ MeV [69,70].[3] To be consistent with the former discussion, the momentum $\boldsymbol{q}$ of the integral in the $K^*\bar{K}$ rest frame is boosted to the f_0, a_0 in the rest frame and one gets a value of $\boldsymbol{q}^*$ given by [34] (for the $f_0(980)\to\pi^+\pi^-$ and similarly for $a_0(980)\to\pi^0\eta$)

[3]The works [66,69,70] rely upon the lowest order chiral Lagrangian for pseudoscalar-pseudoscalar interaction [88]. Extensions to include higher order terms are done in [89,90], and lattice QCD simulations have also done their share to advance in this field [91]. However, one must stress the accuracy of the unitarized approach with the lowest order chiral Lagrangian to produce the $f_0(980)$ and $a_0(980)$ resonances and reproduce experiments where they are observed, as one can see in ϕ decay to $\pi^0\pi^0\gamma$, $\pi^0\eta\gamma$ [92,93], $J/\psi\to\phi\pi\pi$ [94] and the $\chi_{c1}\to\eta\pi^+\pi^-$ [95].

$$\boldsymbol{q}^* = \left[\left(\frac{E_R}{M_{\rm inv}(\pi^-\pi^+)} - 1\right)\frac{\boldsymbol{q}\cdot\boldsymbol{k}}{|\boldsymbol{k}|^2} + \frac{q^0}{M_{\rm inv}(\pi^-\pi^+)}\right]\boldsymbol{k} + \boldsymbol{q}, \qquad (27)$$

with $E_R = \sqrt{M_{\rm inv}(\pi^-\pi^+) + \boldsymbol{k}^2}$, $q^0 = \sqrt{m_K^2 + \boldsymbol{q}^2}$.

In addition, we have made for convenience an approximation $\epsilon_\mu(2k+q)^\mu \to (-1)\boldsymbol{\epsilon}\cdot(2\boldsymbol{k}+\boldsymbol{q})$ in the $K^* \to K\pi$ vertex. This results from neglecting the ϵ^0 component in the longitudinal polarization of the K^*. This is actually a very good approximation for a case like the present one, as explicitly shown in Appendix A of Ref. [18]. The relative error neglecting the ϵ^0 component for a K^* moving with a momentum $\boldsymbol{p}^*$ is given by Eq. (A.6) of Ref. [18],

$$\frac{(E_\pi - E_K)^2}{4|\boldsymbol{p}_\pi|^2}\frac{|\boldsymbol{p}^*|^2}{m^{*2}}, \qquad (28)$$

where E_π, E_K are the π and K energies in the decay of K^* at rest and $\boldsymbol{p}_\pi$ the π momentum in this frame, while m^*, $\boldsymbol{p}^*$ are the mass and the momentum of K^*. At the energy of the triangle singularity of 1420 MeV for the $K^*\bar{K}$ invariant mass we find that $|\boldsymbol{p}^*| = 155$ MeV and Eq. (28) provides 0.57% error.

Then the formalism for the loop diagrams can be done as for the $K^{*0}K^-$ production replacing

$$M_0 \to \tilde{M}_0 t_{K^+K^-,\pi^+\pi^-}; \quad \tilde{M}_0 = g\frac{1}{\sqrt{6}}\frac{1}{4\pi}kt_L,$$
$$N_i \to \tilde{N}_i t_{K^+K^-,\pi^+\pi^-}; \quad \tilde{N}_i = g\frac{1}{\sqrt{3}}\frac{1}{4\pi}kt_L\delta_{i1} \qquad (29)$$

and for K^0K^{*-}, $\tilde{M}_0$ is the same and $\tilde{N}_i$ changes sign.

The combination of the diagram of Fig. 1(b) proceeds in a similar way. The changes are: $t_{K^+K^-\to\pi^+\pi^-}$ is replaced by $t_{K^0\bar{K}^0\to\pi^+\pi^-}$ and the $K^{*-} \to \pi^-\bar{K}^0$ vertex has opposite sign to $K^{*0} \to \pi^-K^+$. Then, the sum of the two terms is taken into account by means of

$$M_0 \to \tilde{M}_0(K^{*0}K^-)t_{K^+K^-,\pi^+\pi^-} - \tilde{M}_0(K^{*-}K^0)t_{K^0\bar{K}^0,\pi^+\pi^-}$$
$$= \tilde{M}_0(K^{*0}K^-)(t_{K^+K^-,\pi^+\pi^-} - t_{K^0\bar{K}^0,\pi^+\pi^-}), \qquad (30)$$

$$N_i \to \tilde{N}_i(K^{*0}K^-)t_{K^+K^-,\pi^+\pi^-} - \tilde{N}_i(K^{*-}K^0)t_{K^0\bar{K}^0,\pi^+\pi^-}$$
$$= \tilde{N}_i(K^{*0}K^-)(t_{K^+K^-,\pi^+\pi^-} + t_{K^0\bar{K}^0,\pi^+\pi^-}). \qquad (31)$$

When we have $\pi^0\eta$ production, as in Fig. 2, the formalism is identical, we only replace $\pi^+\pi^-$ by $\pi^0\eta$ at the end in $t_{K\bar{K}\to m_1'm_2'}$. Next, in order to have isospin conservation and hence proper G-parity states we will solve the $t_{m_1m_2\to m_1'm_2'}$ amplitudes with average masses for the kaons and average masses for the pions and we shall also take average masses for K^* masses in the loop. In this case, we have

$$t_{K^+K^-,\pi^+\pi^-} = t_{K^0\bar{K}^0,\pi^+\pi^-},$$
$$t_{K^+K^-,\pi^0\eta} = -t_{K^0\bar{K}^0,\pi^0\eta}. \qquad (32)$$

Hence in the case of the amplitude M_0 in Eq. (30) and $\pi^+\pi^-$ in the final state we find a cancellation of the amplitudes for diagram of Figs. 1(a) and 1(b). If instead we have $\pi^0\eta$ in the end, the two diagrams of Figs. 2(a) and 2(b) give the same contribution and sum coherently. Conversely, in the N_i term of Eq. (31) the two terms corresponding to Figs. 1(a) and 1(b) add and those of Figs. 2(a) and 2(b) cancel exactly. In summary, the M_0 terms cancel for the production of $f_0(980)$ and add for the production of $a_0(980)$. This is, the $f_0(980)$ production proceeds via the N_i term and the $a_0(980)$ production via the M_0 term. Since $\pi^-f_0(980)$ has negative G-parity and $\pi^-a_0(980)$ positive G-parity, we confirm that the M_0 term in the loop corresponds to positive G-parity and the N_i term to negative G-parity, as we found earlier at the quark level.

Then for $\pi^-f_0(980)$ we will have

$$\bar{\sum}\sum|t|^2 = \bar{L}^{ij}\tilde{N}_i\tilde{N}_j^*g^2|2t_{K^+K^-,\pi^+\pi^-}|^2,$$
$$= \frac{\mathcal{C}^2}{m_\tau m_\nu}\left(E_\tau E_\nu - \frac{1}{3}p^2\right)$$
$$\times\frac{1}{3}\frac{1}{(4\pi)^2}k^2|t_L|^2g^2|2t_{K^+K^-,\pi^+\pi^-}|^2. \qquad (33)$$

Similarly, for the production of $\pi^-a_0(980)$ we will have

$$\bar{\sum}\sum|t|^2 = \bar{L}^{00}\tilde{M}_0\tilde{M}_0^*g^2|2t_{K^+K^-,\pi^0\eta}|^2,$$
$$= \frac{\mathcal{C}^2}{m_\tau m_\nu}(E_\tau E_\nu + p^2)$$
$$\times\frac{1}{6}\frac{1}{(4\pi)^2}k^2|t_L|^2g^2|2t_{K^+K^-,\pi^0\eta}|^2. \qquad (34)$$

where we have taken into account that $p_i\delta_{i1}p_j\delta_{j1}$ is p_x^2 and, when integrated over the phase space, gives rise to $\frac{1}{3}p^2$.

For $\tau^- \to \nu_\tau\pi^-\pi^+\pi^-$ decay, the double differential mass distribution for $M_{\rm inv}(\pi^+\pi^-)$ and $M_{\rm inv}(\pi^-f_0)$ is given by [16]

$$\frac{1}{\Gamma_\tau}\frac{d^2\Gamma}{dM_{\rm inv}(\pi^-f_0)dM_{\rm inv}(\pi^+\pi^-)}$$
$$= \frac{1}{(2\pi)^5}\frac{1}{\Gamma_\tau}kp_\nu'\tilde{q}_{\pi^+}\frac{2m_\tau 2m_\nu}{4M_\tau^2}\bar{\sum}\sum|t|^2, \qquad (35)$$

with k given by Eq. (21) and

$$p_\nu' = \frac{\lambda^{1/2}(m_\tau^2, m_\nu^2, M_{\rm inv}^2(\pi^-f_0))}{2m_\tau},$$
$$\tilde{q}_{\pi^+} = \frac{\lambda^{1/2}(M_{\rm inv}^2(\pi^+\pi^-), m_\pi^2, m_\pi^2)}{2M_{\rm inv}(\pi^+\pi^-)}. \qquad (36)$$

Similarly, for the $\tau^- \to \nu_\tau \pi^- \pi^0 \eta$ decay, we can get the double differential mass distribution for $M_{\rm inv}(\pi^0\eta)$ and $M_{\rm inv}(\pi^- a_0)$.

Note that the term $m_\tau m_\nu$ in the numerator of Eq. (35) cancels the same factor in the denominator of Eqs. (33) and (34). In Eq. (35), we have the factor $\frac{\mathcal{C}^2}{\Gamma_\tau}$, which, as mentioned before, is obtained by means of Eq. (16), and thus we can provide absolute values for the mass distributions.

III. RESULTS

Let us begin by showing in Fig. 5 the contribution of the triangle loop defined in Eq. (26). We plot the real and imaginary parts of t_L, as well as the absolute value as a function of $M_{\rm inv}(\pi^- R)$, with $M_{\rm inv}(R)$ fixed at 985 MeV (R standing for $f_0(980)$ or $a_0(980)$). It can be observed that $\mathrm{Re}(t_T)$ has a peak around 1393 MeV, and $\mathrm{Im}(t_T)$ has a peak around 1454 MeV, and there is a peak for $|t_T|$ around 1425 MeV. As discussed in Refs. [11,18], the peak of the real part is related to the K^*K threshold and the one of the imaginary part, that dominates for the larger $\pi^- R$ invariant masses, to the triangle singularity. Note that around 1420 MeV and above the triangle singularity dominates the reaction.

The origin of the peak in $|t_T|$, and consequently in the $\pi^- R$ mass distribution of the decay, has then the same origin as the peak observed in the COMPASS experiment [6], tentatively branded as a new "$a_1(1420)$" resonance, which however was explained in [3,4] as coming from the same triangle mechanism that we have encountered here. It would be most enlightening to confirm this experimentally in the τ decay reaction to settle discussions around the "$a_1(1420)$" peak.

In Fig. 6, we plot Eq. (35) for the $\tau^- \to \nu_\tau \pi^- \pi^+ \pi^-$ decay, and similarly in Fig. 7 for the $\tau^- \to \nu_\tau \pi^- \pi^0 \eta$ decay as a function of $M_{\rm inv}(R)$, where in both figures we fix $M_{\rm inv}(\pi^- R) = 1317$, 1417, and 1517 MeV and vary $M_{\rm inv}(R)$. We can see that the distribution with largest strength is near $M_{\rm inv}(\pi^- R) = 1417$ MeV. In Fig. 6, we can also see a strong peak in the $\pi^+\pi^-$ mass distribution around 980 MeV for the three different masses of $M_{\rm inv}(\pi^- R)$, corresponding to the $f_0(980)$. Similarly, in Fig. 7 we see the distinctive cusp like $a_0(980)$ peak around 990 MeV for the $\pi^0\eta$ mass distribution.

The signals in Figs. 6 and 7 are what one should aim at in an experiment. Yet, in order to give a branching ratio for what an experimentalist would brand as $\pi^- f_0(980)$ or $\pi^- a_0(980)$ decay, we must integrate the strength of the double differential width in Figs. 6 and 7 over the $\pi^+\pi^-$ or $\pi^0\eta$ invariant masses, respectively. For this we must state the limits of integration, which should be wide enough to cover practically all the strength, without going to other invariant mass regions away from the relevant one. We find a fair range of invariant mass with $M_{\rm inv} \in [920, 1040\ \mathrm{MeV}]$. In this way, we obtain $\frac{1}{\Gamma_\tau}\frac{d\Gamma}{dM_{\rm inv}(\pi^- R)}$ which is shown in Fig. 8. We

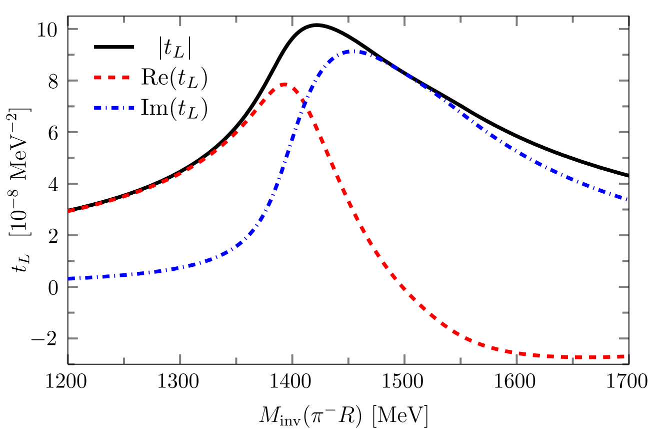

FIG. 5. Triangle amplitude $\mathrm{Re}(t_L)$, $\mathrm{Im}(t_L)$ and $|t_L|$, taking $M_{\rm inv}(R) = 985$ MeV.

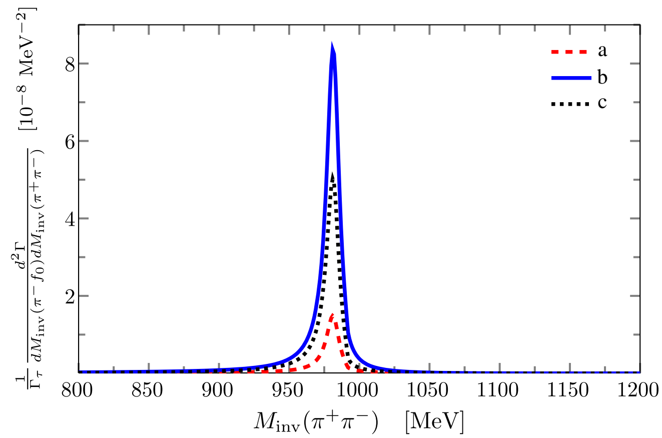

FIG. 6. Double differential width of $\tau^- \to \nu_\tau \pi^- \pi^+ \pi^-$, keeping $M_{\rm inv}(\pi^- f_0)$ fixed to three values. Lines a, b and c show the values at $M_{\rm inv}(\pi^- f_0)$ 1317, 1417, and 1517 MeV, respectively, plotted vs $M_{\rm inv}(\pi^+\pi^-)$.

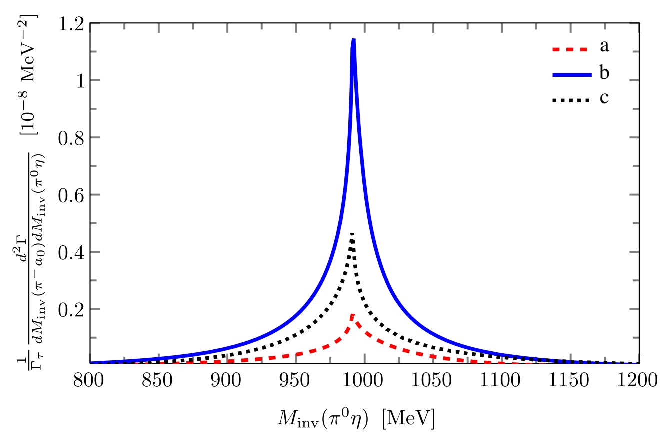

FIG. 7. Double differential width of $\tau^- \to \nu_\tau \pi^- \pi^0 \eta$, keeping $M_{\rm inv}(\pi^- a_0)$ fixed to three values. Lines a, b and c show the values at $M_{\rm inv}(\pi^- a_0)$ 1317, 1417, and 1517 MeV, respectively, plotted vs $M_{\rm inv}(\pi^0\eta)$.

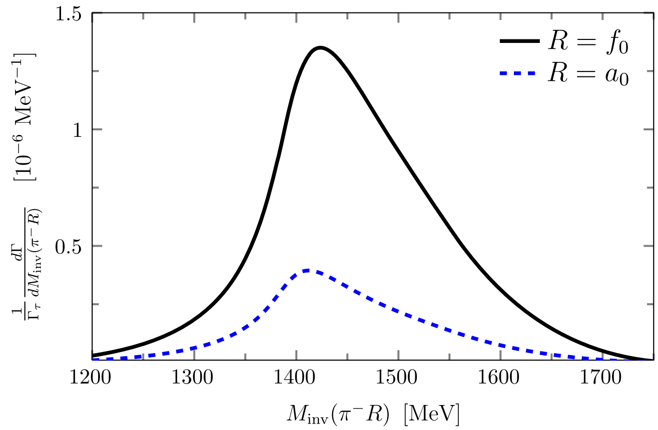

FIG. 8. The mass distribution for $\pi^- R$ ($R = f_0$, a_0). The solid line for $\tau^- \to \nu_\tau \pi^- \pi^+ \pi^-$ as a function of $M_{\rm inv}(\pi^- R)$ with $R \equiv f_0(980)$ measured in the $\pi^+\pi^-$ decay mode; dashed line for $\tau^- \to \nu_\tau \pi^- \pi^0 \eta$ as a function of $M_{\rm inv}(\pi^- R)$ with $R \equiv a_0(980)$ measured in the $\pi^0\eta$ decay mode.

see a clear peak of the distribution around 1423 MeV for $\pi^- f_0(980)$ production and 1412 MeV for $\pi^- a_0(980)$ production.

Integrating $\frac{d\Gamma}{dM_{\rm inv}(\pi^- R)}$ over $M_{\rm inv}(\pi^- R)$ in Fig. 8, we obtain the branching fractions

$$\begin{aligned} &\mathcal{B}(\tau^- \to \nu_\tau \pi^- f_0(980); f_0(980) \to \pi^+\pi^-) \\ &\quad = (2.6 \pm 0.5) \times 10^{-4}, \\ &\mathcal{B}(\tau^- \to \nu_\tau \pi^- a_0(980); a_0(980) \to \pi^0\eta) \\ &\quad = (7.1 \pm 1.4) \times 10^{-5}. \end{aligned} \tag{37}$$

Since the rate of $f_0 \to \pi^0\pi^0$ is one half that of $f_0 \to \pi^+\pi^-$, we can write

$$\mathcal{B}(\tau^- \to \nu_\tau \pi^- f_0(980)) = (3.9 \pm 0.8) \times 10^{-4}. \tag{38}$$

The errors in these numbers count only the relative error of the branching ratio of Eq. (15). These numbers are within measurable range, since branching ratios of 10^{-5} and smaller are quoted in the PDG for τ decays [7].

The rates of 10^{-4} could look small compared to the background for $\pi^-\pi^+\pi^-\nu_\tau$ decay with a branching ratio of $(9.31 \pm 0.05) \times 10^{-2}$ [7] or $\pi^-\pi^0\eta\nu_\tau$ with a branching ratio of $(1.39 \pm 0.07) \times 10^{-3}$ [7]. Yet, the signals for $f_0(980)$ and $a_0(980)$ are very distinct and a special search for these modes should lead to the identification of the decays studied here. To put this in a broader context let us recall that the $\tau^- \to \nu_\tau f_1(1285)\pi^-$ decay has been identified with a branching ratio of $(3.9 \pm 0.5) \times 10^{-4}$ [7], similar to what we obtain here. Even more, the peculiar channel $\tau^- \to \nu_\tau f_1(1285)\pi^- \to \nu_\tau \pi^- K_s^0 K_s^0 \pi^0$ has been identified with a branching ratio of $(6.8 \pm 1.5) \times 10^{-6}$ [7]. With this present state of the art, the measurements of the reactions proposed should be accessible and the planned updates of some of the facilities and possible future ones, can only make it easier.

One might worry about a possible interference between the terms of the dominant mechanism in $\tau^- \to \nu_\tau \pi^-\pi^+\pi^-$ ($a_1(1260) \to \pi^-\rho^0 \to \pi^-\pi^+\pi^-$) and those of the present one. One can recall general arguments of phase space, since our mechanism concentrates on a narrow region of $M_{\rm inv}(\pi^-\pi^+\pi^-)$ and $M_{\rm inv}(\pi^+\pi^-)$, while the other mechanism concentrates in a very different region. In the limit of very narrow widths of resonances in the two mechanisms, there is no interference between them. In our case, the $f_0(980)$ and $a_0(980)$ are quite narrow but not the ρ and $a_1(1260)$. Yet, there is usually some memory of the lack of interference in the realistic cases. However, in the present case there is a more compelling argument. Indeed, the $\pi^+\pi^-$ from the $f_0(980)$ come in s-wave, while those from the ρ^0 come in p-wave. In addition, the π^- from K^* decay comes in p-wave while the one from $a_1(1260) \to \pi^-\rho^0$ comes in s-wave. Upon angle integration in the phase space the interference term disappears. Finally, we should also note, that, while the detection of π^0 is always more problematic than for charged pions, the detection of $\pi^0\pi^0$ in decays is common place nowadays [96], and concretely coming from the $f_0(980)$ is done in the $\phi \to \gamma\pi^0\pi^0$ in [97]. Since the ρ^0 cannot decay to $\pi^0\pi^0$, the $\pi^0\pi^0$ decay mode of the $f_0(980)$ is always cleaner than that of $\pi^+\pi^-$. The reasons exposed above tell us that in the phase space where we investigate the $\tau^- \to \nu_\tau \pi^- f_0(980)$, the mechanisms different to the one we have studied, should just provide a background. Similar arguments can be used for the case of $a_0(980)$ decay to $\pi^0\eta$.

Finally, even if it is unclear that it is related to our mechanism, we should mention that in Ref. [98] claims are made that the $\tau^- \to \nu_\tau \pi^-\pi^+\pi^-$ decay requires a small contribution of an "$a_1(1420)$" resonance in the $\pi^-\pi^+\pi^-$ invariant mass, decaying to π^- and $\pi\pi s$-wave. The $\pi\pi s$-wave is taken in [98] as corresponding to the σ ($f_0(500)$), but it is also mentioned that it could equally correspond to $f_0(980)$. Yet, these results are very qualitative and should be gauged against other detailed work described above.

IV. CONCLUSIONS

We have made a study of the $\tau^- \to \nu_\tau \pi^- f_0(980)$ and $\tau^- \to \nu_\tau \pi^- a_0(980)$ reactions from the perspective that the $f_0(980)$ and $a_0(980)$ are dynamically generated resonances from the interaction of pseudoscalar mesons in coupled channels. We showed that the main mechanism for these processes proceeds via $\tau \to \nu_\tau K^{*0} K^-$ ($K^0 K^{*-}$) followed by $\bar{K}^* \to \pi^- K$ and the posterior fusion of $K\bar{K}$ to produce either the $f_0(980)$ or $a_0(980)$ states. This triangle mechanism has a peculiarity since it develops a triangle singularity at $M_{\rm inv}(\pi^- R) \simeq 1420$ MeV ($R \equiv f_0$ or a_0), and the

$M_{\rm inv}(\pi^- R)$ distribution shows a peak around this energy, which has then the same origin as the explanations given in [3,4] for the COMPASS peak in $\pi f_0(980)$ that was initially presented as the new resonance "$a_1(1420)$". It would be most instructive to have the experiment performed to see if such peak indeed appears, which would help clarify the issue around the "$a_1(1420)$" peak.

On the other hand, we make predictions which are tied to the way the $f_0(980)$ and $a_0(980)$ resonances are generated and again the observations will bring extra information on the nature of these low-lying scalar states.

The mechanism requires the use of the amplitude for the $\tau \to \nu_\tau K^{*0} K^-$ reaction in a way suited to the calculation of the loop function of the triangle mechanism. This task was made efficient and easily manageable thanks to the formalism developed in [57,58] which provides two amplitudes with given G-parity in terms of the third components of the K^{*0} spin. Since $\pi^- f_0(980)$ and $\pi^- a_0(980)$ have negative and positive G-parity, respectively, the formalism filtered just one of these amplitudes for either reaction, with the subsequent economy and clarity in the formulation.

We could provide absolute values for the mass distributions and final branching ratios by using the experimental branching ratio of the $\tau \to \nu_\tau K^{*0} K^-$ reaction. Hence, our predictions are free of intrinsic uncertainties that *ab initio* microscopic models unavoidably have, and which would be magnified in this problem where final state interaction of hadrons is at work.

With the reliable predictions of our approach, we find final branching ratios of $\pi^- f_0(980)$ and $\pi^- a_0(980)$ of about 4×10^{-4} and 7×10^{-5}, respectively. These rates are well within measurable range and we can only encourage the performance of the experiments.

As we discussed in the Introduction, there are measurements for the $\tau^- \to \nu_\tau \pi^- \pi^+ \pi^-$ and $\tau^- \to \nu_\tau \pi^- \pi^0 \eta$. However, none of them has addressed the region of $M_{\rm inv}(\pi^- \pi^+ \pi^-) \sim 1420$ MeV together with $M_{\rm inv}(\pi^+ \pi^-)$, $M_{\rm inv}(\pi^0 \eta)$ around the $f_0(980)$ and $a_0(980)$ regions. The present work should present a justification for future experiments in the new updated Belle II or the projected facilities at Hefei and Novosibirsk.

ACKNOWLEDGMENTS

L. R. D. acknowledges the support from the National Natural Science Foundation of China (Grant No. 11575076) and the State Scholarship Fund of China (No. 201708210057). Q. X. Y. acknowledges the support from the National Natural Science Foundation of China (Grants No. 11775024 and No. 11575023). This work is partly supported by the Spanish Ministerio de Economia y Competitividad and European FEDER funds under Contracts No. FIS2017-84038-C2-1-P B and No. FIS2017-84038-C2-2-P B, the Generalitat Valenciana in the program Prometeo II-2014/068, and the project Severo Ochoa of IFIC, SEV-2014-0398 (E. O.).

[1] L. D. Landau, Nucl. Phys. **13**, 181 (1959).
[2] S. Coleman and R. E. Norton, Nuovo Cimento **38**, 438 (1965).
[3] M. Mikhasenko, B. Ketzer, and A. Sarantsev, Phys. Rev. D **91**, 094015 (2015).
[4] F. Aceti, L. R. Dai, and E. Oset, Phys. Rev. D **94**, 096015 (2016).
[5] X. H. Liu, M. Oka, and Q. Zhao, Phys. Lett. B **753**, 297 (2016).
[6] C. Adolph *et al.* (COMPASS Collaboration), Phys. Rev. Lett. **115**, 082001 (2015).
[7] M. Tanabashi *et al.* (Particle Data Group), Phys. Rev. D **98**, 030001 (2018).
[8] D. Barberis *et al.* (WA102 Collaboration), Phys. Lett. B **440**, 225 (1998).
[9] V. R. Debastiani, F. Aceti, W. H. Liang, and E. Oset, Phys. Rev. D **95**, 034015 (2017).
[10] J. J. Xie, L. S. Geng, and E. Oset, Phys. Rev. D **95**, 034004 (2017).
[11] L. R. Dai, R. Pavao, S. Sakai, and E. Oset, Phys. Rev. D **97**, 116004 (2018).
[12] A. P. Szczepaniak, Phys. Lett. B **747**, 410 (2015).
[13] A. P. Szczepaniak, Phys. Lett. B **757**, 61 (2016).
[14] A. E. Bondar and M. B. Voloshin, Phys. Rev. D **93**, 094008 (2016).
[15] A. Pilloni, C. Fernández-Ramírez, A. Jackura, V. Mathieu, M. Mikhasenko, J. Nys, and A. P. Szczepaniak (JPAC Collaboration), Phys. Lett. B **772**, 200 (2017).
[16] R. Pavao, S. Sakai, and E. Oset, Eur. Phys. J. C **77**, 599 (2017).
[17] X. H. Liu and U. G. Meißner, Eur. Phys. J. C **77**, 816 (2017).
[18] S. Sakai, E. Oset, and A. Ramos, Eur. Phys. J. A **54**, 10 (2018).
[19] L. Roca and E. Oset, Phys. Rev. C **95**, 065211 (2017).
[20] D. Samart, W. H. Liang, and E. Oset, Phys. Rev. C **96**, 035202 (2017).
[21] J. J. Wu, X. H. Liu, Q. Zhao, and B. S. Zou, Phys. Rev. Lett. **108**, 081803 (2012).
[22] F. Aceti, W. H. Liang, E. Oset, J. J. Wu, and B. S. Zou, Phys. Rev. D **86**, 114007 (2012).
[23] X. G. Wu, J. J. Wu, Q. Zhao, and B. S. Zou, Phys. Rev. D **87**, 014023 (2013).
[24] X. H. Liu and G. Li, Eur. Phys. J. C **76**, 455 (2016).
[25] E. Wang, J. J. Xie, W. H. Liang, F. K. Guo, and E. Oset, Phys. Rev. C **95**, 015205 (2017).

[26] J. J. Xie and F. K. Guo, Phys. Lett. B **774**, 108 (2017).
[27] Z. Cao and Q. Zhao, arXiv:1711.07309.
[28] W. H. Liang, S. Sakai, J. J. Xie, and E. Oset, Chin. Phys. C **42**, 044101 (2018).
[29] V. R. Debastiani, S. Sakai, and E. Oset, arXiv:1809.06890.
[30] B. Aubert *et al.* (*BABAR* Collaboration), Phys. Rev. Lett. **115**, 072001 (2015).
[31] M. Mikhasenko, arXiv:1507.06552.
[32] X. H. Liu, Q. Wang, and Q. Zhao, Phys. Lett. B **757**, 231 (2016).
[33] F. K. Guo, U. G. Meißner, W. Wang, and Z. Yang, Phys. Rev. D **92**, 071502 (2015).
[34] M. Bayar, F. Aceti, F. K. Guo, and E. Oset, Phys. Rev. D **94**, 074039 (2016).
[35] R. Barate *et al.* (ALEPH Collaboration), Eur. Phys. J. C **4**, 409 (1998).
[36] I. M. Nugent, Ph.D. thesis, SLAC-R-936, 2009.
[37] R. A. Briere *et al.* (CLEO Collaboration), Phys. Rev. Lett. **90**, 181802 (2003).
[38] B. Aubert *et al.* (*BABAR* Collaboration), Phys. Rev. Lett. **100**, 011801 (2008).
[39] M. J. Lee *et al.* (Belle Collaboration), Phys. Rev. D **81**, 113007 (2010).
[40] I. M. Nugent, T. Przedzinski, P. Roig, O. Shekhovtsova, and Z. Was, Phys. Rev. D **88**, 093012 (2013).
[41] K. Inami *et al.* (Belle Collaboration), Phys. Lett. B **672**, 209 (2009).
[42] D. Buskulic *et al.* (ALEPH Collaboration), Z. Phys. C **74**, 263 (1997).
[43] M. Artuso *et al.* (CLEO Collaboration), Phys. Rev. Lett. **69**, 3278 (1992).
[44] M. G. Bowler, Phys. Lett. B **182**, 400 (1986).
[45] N. Isgur, C. Morningstar, and C. Reader, Phys. Rev. D **39**, 1357 (1989).
[46] G. Colangelo, M. Finkemeier, and R. Urech, Phys. Rev. D **54**, 4403 (1996).
[47] D. G. Dumm, P. Roig, A. Pich, and J. Portoles, Phys. Lett. B **685**, 158 (2010).
[48] Z. Was and J. Zaremba, Eur. Phys. J. C **75**, 566 (2015); **76**, 465(E) (2016).
[49] J. J. Sanz-Cillero and O. Shekhovtsova, J. High Energy Phys. 12 (2017) 080.
[50] Z. H. Guo, Phys. Rev. D **78**, 033004 (2008).
[51] A. Pich, Phys. Lett. B **196**, 561 (1987).
[52] D. G. Dumm and P. Roig, Phys. Rev. D **86**, 076009 (2012).
[53] A. Pich, Prog. Part. Nucl. Phys. **75**, 41 (2014).
[54] J. Portoles, Nucl. Phys. B, Proc. Suppl. **169**, 3 (2007).
[55] M. Mikhasenko, A. Pilloni, A. Jackura, M. Albaladejo, C. Fernández-Ramírez, V. Mathieu, J. Nys, A. Rodas, B. Ketzer, and A. P. Szczepaniak (JPAC Collaboration), Phys. Rev. D **98**, 096021 (2018).
[56] C. Leroy and J. Pestieau, Phys. Lett. **72B**, 398 (1978).
[57] L. R. Dai, R. Pavao, S. Sakai, and E. Oset, Eur. Phys. J. A, arXiv:1805.04573.
[58] L. R. Dai and E. Oset, Eur. Phys. J. A **54**, 219 (2018).
[59] Q. Luo and D. R. Xu, *Proceedings of the 9th International Particle Accelerator Conference*, https://doi.org/10.18429/JACoW-IPAC2018-MOPML013.
[60] S. Eidelman, Nucl. Part. Phys. Proc. **260**, 238 (2015).
[61] E. Kou *et al.* (Belle II Collaboration), arXiv:1808.10567.
[62] E. Oset and L. Roca, Phys. Lett. B **782**, 332 (2018).
[63] L. Roca, E. Oset, and J. Singh, Phys. Rev. D **72**, 014002 (2005).
[64] Y. Zhou, X. L. Ren, H. X. Chen, and L. S. Geng, Phys. Rev. D **90**, 014020 (2014).
[65] M. K. Volkov, A. A. Pivovarov, and A. A. Osipov, Eur. Phys. J. A **54**, 61 (2018).
[66] J. A. Oller and E. Oset, Nucl. Phys. **A620**, 438 (1997); **A652**, 407(E) (1999).
[67] J. Nieves and E. Ruiz Arriola, Nucl. Phys. **A679**, 57 (2000).
[68] N. Kaiser, Eur. Phys. J. A **3**, 307 (1998).
[69] W. H. Liang and E. Oset, Phys. Lett. B **737**, 70 (2014).
[70] J. J. Xie, L. R. Dai, and E. Oset, Phys. Lett. B **742**, 363 (2015).
[71] M. P. Locher, V. E. Markushin, and H. Q. Zheng, Eur. Phys. J. C **4**, 317 (1998).
[72] L. Micu, Nucl. Phys. **B10**, 521 (1969).
[73] A. Le Yaouanc, L. Oliver, O. Pène, and J. C. Raynal, Phys. Rev. D **8**, 2223 (1973).
[74] E. Santopinto and R. Bijker, Phys. Rev. C **82**, 062202 (2010).
[75] B. C. Barish and R. Stroynowski, Phys. Rep. **157**, 1 (1988).
[76] F. Mandl and G. Shaw, *Quantum Field Theory* (John Wiley & Sons, Hoboken, 1984).
[77] T. E. Coan *et al.* (CLEO Collaboration), Phys. Rev. Lett. **92**, 232001 (2004).
[78] J. J. Gomez-Cadenas, M. C. Gonzalez-Garcia, and A. Pich, Phys. Rev. D **42**, 3093 (1990).
[79] M. Davier, S. Descotes-Genon, A. Hocker, B. Malaescu, and Z. Zhang, Eur. Phys. J. C **56**, 305 (2008).
[80] D. G. Dumm, P. Roig, A. Pich, and J. Portoles, Phys. Rev. D **81**, 034031 (2010).
[81] S. Schael *et al.* (ALEPH Collaboration), Phys. Rep. **421**, 191 (2005).
[82] C. N. Yang and R. L. Mills, Phys. Rev. **96**, 191 (1954).
[83] S. Gasiorowicz and D. A. Geffen, Rev. Mod. Phys. **41**, 531 (1969).
[84] J. Schechter and Y. Ueda, Phys. Rev. **188**, 2184 (1969).
[85] U. G. Meissner, Phys. Rep. **161**, 213 (1988).
[86] F. Aceti, J. M. Dias, and E. Oset, Eur. Phys. J. A **51**, 48 (2015).
[87] D. Gamermann, J. Nieves, E. Oset, and E. Ruiz Arriola, Phys. Rev. D **81**, 014029 (2010).
[88] J. Gasser and H. Leutwyler, Ann. Phys. (N.Y.) **158**, 142 (1984).
[89] Z. H. Guo, L. Liu, U. G. Meißner, J. A. Oller, and A. Rusetsky, Phys. Rev. D **95**, 054004 (2017).
[90] F. K. Guo, C. Hanhart, U. G. Meißner, Q. Wang, Q. Zhao, and B. S. Zou, Rev. Mod. Phys. **90**, 015004 (2018).
[91] R. A. Briceno, J. J. Dudek, and R. D. Young, Rev. Mod. Phys. **90**, 025001 (2018).
[92] E. Marco, S. Hirenzaki, E. Oset, and H. Toki, Phys. Lett. B **470**, 20 (1999).

[93] J. E. Palomar, L. Roca, E. Oset, and M. J. Vicente Vacas, Nucl. Phys. **A729**, 743 (2003).
[94] L. Roca, J. E. Palomar, E. Oset, and H. C. Chiang, Nucl. Phys. **A744**, 127 (2004).
[95] W. H. Liang, J. J. Xie, and E. Oset, Eur. Phys. J. C **76**, 700 (2016).
[96] V. Crede *et al.* (CBELSA/TAPS Collaboration), Phys. Rev. C **80**, 055202 (2009).
[97] M. N. Achasov *et al.* (SND Collaboration), Phys. Lett. B **440**, 442 (1998).
[98] P. Lichard, arXiv:1703.06315.